UNIVERSIDAD NACIONAL DE COLOMBIA
SEDE MEDELLÍN
FACULTAD DE MINAS

DYNA
http://dyna.medellin.unal.edu.co/

Radiation forces study of a Laguerre Gaussian beam type TEM_{01}^{*} on a dielectric sphere in the Rayleigh scattering regime

Darby Paez-Amaya, Martha Lucía Molina-Prado & Néstor Alonso Arias-Hernández

Grupo de Óptica Moderna, Departamento de Física y Geología, Universidad de Pamplona, Pamplona, Colombia. darby.paez@unipamplona,edu.co, marlumopra@unipamplona.edu.co, nesariher@unipamplona.edu.co

Received: August 6th, de 2018. Received in revised form: May 7th, 2019. Accepted: May 24th, 2019.

Abstract
From the invention of the Optical Tweezer (OT) in 1986, these devices have been considered as high-level tools for research in the areas such as biology and microbiology. A theoretical study obtaining equations for gradient and scattering forces that exert an OT when the illumination beam is a doughnut-shaped mode TEM_{01}^{*} linearly polarized is realized. This work focuses on the behavior of radiation forces on a dielectric sphere in the Rayleigh regime. In order to facilitate the phenomenological analysis of the behavior of the radiation forces a graphical user interface is created.

Keywords: optical tweezer; beam doughnut-shaped; Rayleigh's regime.

Estudio de las fuerzas de radiación de un haz Laguerre Gaussiano modo TEM_{01}^{*} sobre una esfera dieléctrica en el régimen de dispersión de Rayleigh

Resumen
A partir de la invención de la pinza óptica en 1986, estos dispositivos se han considerado como herramientas de alto nivel para la investigación, destacándose en áreas como la biología y la microbiología. En este trabajo se realiza un estudio teórico, obteniendo expresiones para las fuerzas de *Gradiente y Scattering* que ejerce una pinza óptica, cuando el haz de iluminación es un modo doughnut-shaped tipo TEM_{01}^{*} polarizado linealmente. Este trabajo se enfoca en calcular el comportamiento de las fuerzas de la radiación sobre una esfera dieléctrica en el régimen de Rayleigh. Con el fin de facilitar el análisis fenomenológico del comportamiento de las fuerzas de captura, se construye una Interfaz Gráfica de Usuario.

Palabras clave: pinza óptica; haz doughnut-shaped; régimen de Rayleigh.

1. Introduction

The operation of the OT, part of the idea that light exerts pressure on material objects, phenomenon called radiation pressure. The first speculations on the existence of the phenomenon go back to the XVII century with the astronomical observations of Johannes Kepler, approximately in the year 1619, and later with theoretical contributions of James Clerk Maxwell in 1873; the first observations and preliminary documentation of the radiation pressure observed in 1901 by E.F. Nichols y G.F. Hull. However, with since of quantum mechanics, with Max Planck and Albert Einstein and with the invention of the laser, that is in 1970 it was possible to obtain the experimental proof where the laser light has the capacity of moving and physically holding microscopic objects by Arthur Ashkin [1]. With the invention of OT, a window been opened for the application it several areas like Atomic Physics, Nanotechnology, Genetics, Biology and Microbiology, because with OT it is possible to individually analyze the microorganisms, allowing to measure mechanical forces and elastic properties [2-3]. In addition to its ability to hold and move microscopic objects without direct contact and

How to cite: Paez-Amaya, D., Molina-Prado, M.L. and Arias-Hernández, N.A., Radiation forces study of a Laguerre Gaussian beam type TEM_{01}^{*} on a dielectric sphere in the Rayleigh scattering regime. DYNA, 86(210), pp. 187-193, July - September, 2019.

exerting small forces around pN. However, conventional OT with Gaussian capture beam and many other limitations: The particles are trapped in the zone of high intensity of the beam and therefore, susceptible to optical damage of the sample (*opticution*) [4], due to absorption heating, plus of attracting multiple particles in the same trap, requiring the use of diluted samples and lasers with specific wavelengths.

Currently, the use of optical vortex trapping beams has been increasing and many applications have been found [5-9]. Compared to regular Gaussian beams, doughnut-shaped modes, such as TEM_{01}^{*}, are suitable to avoid laser-induced heating and optical damage since the intensity profile drops to zero at the optical axis [6,9].

The prediction of the optical forces that are present in optical trapping is a current problem in continuous evolution. Now, with the use of complex beam like TEM_{01}^{*} makes the problem even more complex. In this paper, we obtained math expressions for the radiation forces in the Rayleigh's regime, in order to predict the behavior of a dielectric sphere, under illumination of TEM_{01}^{*} mode linearly polarized.

2. Theoretical analysis

To explain the behavior of the radiation forces, present in an OT when capturing a micrometer object, there are some methods; in particular, the so-called Approximate Methods, these methods have proven to be useful in the field of OT due to the theoretical and phenomenological analysis they provide. One of these approximate methods is Rayleigh's Dipolar Theory [10], which may be lower in the sense of some approximations, which is smaller than the wavelength of the capture beam. This method consists in consider light as electromagnetic waves and analyzer the behavior of the radiation sphere when it interacts with the capture radiation. As the size of the sphere is considered small, the electromagnetic field incident on the sphere is considered homogeneos, allowing that the dielectric sphere it is behavior as a puntual dielectric dipole.

By electric field action an electric dipole moment is induced in the sphere that has the form [10-12]:

$$\boldsymbol{p}(\mathrm{r},t) = 4\pi n_m^2 \varepsilon_0 a^3 \left(\frac{m^2-1}{m^2+2}\right) \boldsymbol{E}(\mathrm{r},t), \tag{1}$$

Where n_m is the refractive index of the medium, ϵ_0 is the electric permittivity of vacuum, a is the radius of sphere, $m = n_p/n_m$ is the refractive index of the sphere (n_p) relative to environment (n_m) and $\mathbf{E}(r,t)$ is the electric field of the incident radiation. The first force considering is a consequence of the interaction of the electric and magnetic fields of the light beam on the sphere and is exactly the Lorentz's force.

In order to find the mathematical form of the force, it is necessary to calculate the electric and magnetic force on the sphere, taking as an observation point the beam waist and thus obtaining an expression for the force because of the interaction of both fields on the regions positively and negatively charged in the dielectric sphere, adding up both contributions and expressing in terms of electric dipole momento $\boldsymbol{p}$, it is possible to say that:

$$\boldsymbol{F}_{Neta}(r,t) = (\boldsymbol{p}.\boldsymbol{\nabla})\boldsymbol{E}(r,t) + \frac{d\boldsymbol{p}}{dt} \times \boldsymbol{B}(r,t). \tag{2}$$

Substituting the equation (1) in (2), applying vector identities and because of the electric and magnetic field changes rapidly in time, the temporary average of them is calculated (see Appendix), obtaining:

$$\langle \boldsymbol{F}_{Neta}(r,t)\rangle_T = \boldsymbol{F}_G(r) = \frac{2\pi n_m a^3}{c}\left[\frac{m^2-1}{m^2+2}\right]\boldsymbol{\nabla} I(r). \tag{3}$$

Where c is the light velocity of vacuum and $\boldsymbol{\nabla} I(r)$ is the Gradient of the intensity light beam; thus, the equation (3) is called *Gradient Force*.

If is have in account the description of the Laguerre beams [14-15], and considering the parameters beam, is possible writing the linearly polarized electric field in direction $\hat{x}$ as;

$$\begin{aligned}\boldsymbol{E}^{LG}(r,\phi,z) = &\sqrt{\frac{2p!}{\pi(p+l)!}}\frac{E_0}{w(z)}\left(\frac{r\sqrt{2}}{w(z)}\right)^l L_p^l\left(\frac{2r^2}{w^2(z)}\right)\\ &\times exp\left[-\frac{r^2}{w^2(z)}\right] exp\left[-\frac{ikr^2}{2R(z)}\right] exp[-il\phi]\\ &\times exp[i(2p+l+1)\xi(z)]\hat{x}\,.\end{aligned} \tag{4}$$

where r,ϕ,z are cylindrical coordinates, E_0 is the amplitude of electric field and the parameters of the beam: $w(z)$ is radius of the beam, $R(z)$ is the radius of curvature and therefore, it is the description of how the wavefront envolves the propagation along the axis, k is the wave number in the medium and $\xi(z)$ is the Gouy's phase change which is the delay of the phase of beam relative to a wave plane [16].

The capture beam that considered is the doughnut-shaped mode type TEM_{01}^{*}. Substituting in the equation (4) the radial index as $p = 0$, this is obtained the electric field for this beam, which is related with its radial distribution and azimuth index $l = 1$ is his helical phase. Later we calculate the intensity of the light beam [17], and replacing in equation (3) we find the shape of the *Gradient force* in the three normal coordinates, defined in this way $(\tilde{x},\tilde{y},\tilde{z}) = \left(\frac{x}{w_0},\frac{y}{w_0},\frac{z}{kw_0^2}\right)$:

$$\begin{aligned}\boldsymbol{F}_{G,x}(r) = &\frac{8\pi n_m a^3\tilde{x}}{cw_0}\left(\frac{m^2-1}{m^2+2}\right)\left(\frac{2P}{\pi w_0^2}\right)\left(\frac{1}{[1+(2\tilde{z})^2]^2}\right)\\ &\times exp\left[-\frac{2(\tilde{x}^2+\tilde{y}^2)}{[1+(2\tilde{z})^2]}\right]\left[1-\frac{2(\tilde{x}^2+\tilde{y}^2)}{[1+(2\tilde{z})^2]}\right]\hat{x},\end{aligned} \tag{5}$$

$$\begin{aligned}\boldsymbol{F}_{G,y}(r) = &\frac{8\pi n_m a^3\tilde{y}}{cw_0}\left(\frac{m^2-1}{m^2+2}\right)\left(\frac{2P}{\pi w_0^2}\right)\left(\frac{1}{[1+(2\tilde{z})^2]^2}\right)\\ &\times exp\left[-\frac{2(\tilde{x}^2+\tilde{y}^2)}{[1+(2\tilde{z})^2]}\right]\left[1-\frac{2(\tilde{x}^2+\tilde{y}^2)}{[1+(2\tilde{z})^2]}\right]\hat{y},\end{aligned} \tag{6}$$

$$\boldsymbol{F}_{G,z}(r) = -\frac{2\pi n_m a^3}{c}\left(\frac{m^2-1}{m^2+2}\right)\left(\frac{2P}{\pi w_0^2}\right) \times \frac{32\tilde{z}/kw_0^2\,(\tilde{x}^2+\tilde{y}^2)}{[1+(2\tilde{z})^2]^3}\, exp\left[-\frac{2(\tilde{x}^2+\tilde{y}^2)}{[1+(2\tilde{z})^2]}\right] \times \left[1-\frac{(\tilde{x}^2+\tilde{y}^2)}{[1+(2\tilde{z})^2]}\right]\hat{z}, \quad (7)$$

Where, P is the power of the laser beam and w_0 is the radius of the beam waist.

The second force that is takes in account arises from the scattering of the light when the electromagnetic wave incise on the sphere. The dipole oscillates and acts as a source of secondary emission, that emit electromagnetic waves in all directions, due to the oscillating nature of the electric and magnetic fields, and due at size significantly small of the sphere with respect at the wavelenght of the light the dipole oscillates synchronically with the field. As the medium that around of the sphere is considered homogeneous, the resulting propagations is in the direction of the incident wave.

If takes in account the interchanged of the lineal momentum of the beam at the dipole, the transverse section of scattering and the intensity of capture beam, the shaped of the *Scattering Force* is obtained [10-12]:

$$\boldsymbol{F}_{Scatt}(r) = \frac{n_m I(r)}{c}\sigma_s\hat{z}, \quad (8)$$

where σ_s is denomined cross section of scattering, being this a perpendicular plane to the propagation vector of the scattered wave and for a dielectric sphere that scatters light of isotropic form, has the form [18]:

$$\sigma_s = \frac{8}{3}\pi k^4 a^6\left|\frac{m^2-1}{m^2+2}\right|^2. \quad (9)$$

Taking the form of intensity of the capture beam TEM_{01}^* and cross section of the scattering, equation (9); is possible writing of the *Scattering force* in function of normalized coordinates as:

$$\boldsymbol{F}_{Scatt}(r) = \frac{8n_m\pi k^4 a^6}{3c}\left|\frac{m^2-1}{m^2+2}\right|^2\left(\frac{2P}{\pi w_0^2}\right) \times \left[\frac{2(\tilde{x}^2+\tilde{y}^2)}{[1+(2\tilde{z})^2]^2}\right] exp\left[-\frac{2(\tilde{x}^2+\tilde{y}^2)}{[1+(2\tilde{z})^2]}\right]\hat{z}. \quad (10)$$

3. Results

Through the equations (5), (6), (7) and (10) it is possible to analyze the behavior of the *Gradient force* and the *Scattering force* in the capture of a sphere of radius $a = 5nm$, with refractive index $n_p = 1{,}592$, which is immersed in a medium of refractive index $n_m = 1{,}332$, using a Gaussian Laguerre capture beam polarized linearly doughnut-shaped mode type TEM_{01}^* on the axe x with a power $P = 100mW$ and a wavelength $\lambda = 514{,}5nm$ and a beam waist $w_0 = 5\mu m$.

The results obtained for the component in x of the *Gradient force* as is observed in the Fig. 1. In addition to the transverse profile in x of the intensity of the beam TEM_{01}^* (dotted line). Intensity profile has been given an adequate maximum value, in order to give clarity to the behavior of said force in the beam intensity zones.

In the Fig. 1, is possible to observe that for values $-1 < \tilde{x} < -0{,}7$, the *Gradient force* take positive values, which indicating that it is exerts a force that sends the sphere towards the zone of greater intensity $\tilde{x} \approx -0{,}7$ and for values $-0{,}7 < \tilde{x} < 0$ when the sphere it outside of the greater intensity zone but close dark central area of the beam, the *Gradient force* take negative values, indicating that it exerts a force that sends the sphere towards the zone of greater intensity $\tilde{x} \approx -0{,}7$. The same behavior is evidenced for zones where $\tilde{x} > 0$. Finally, it is possible to conclude that there is a restorative behavior of the transverse nature x of the *Gradient force*, that is present in the location of the dielectric sphere in the zones of greater intensity of the beam TEM_{01}^*. Furthermore, it should be noted that as shown in Fig. 1, the *Gradient Force* is not present in the dark zone of the beam, because the force depends on the intensity of the beam.

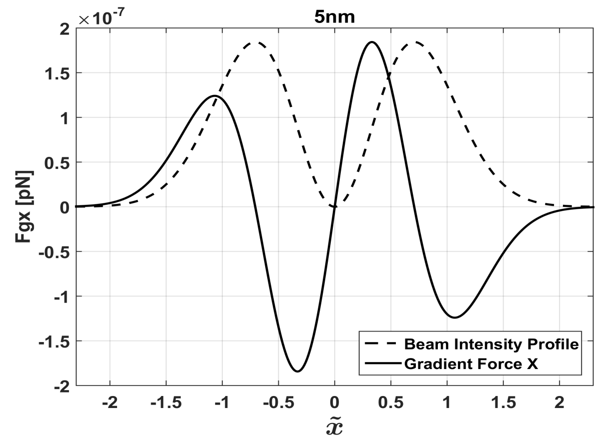

Figure 1. Transverse Component x of the Gradient Force for a dielectric sphere of radius $5nm$.
Source: The Authors.

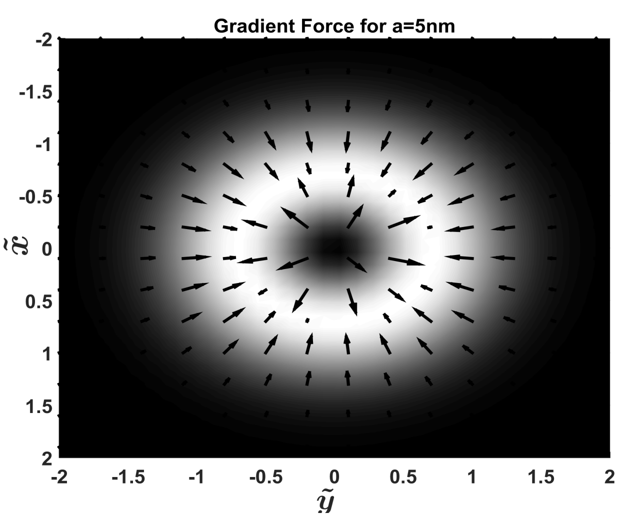

Figure 2. Transverse Plane xy of the *Gradient Force* for a dielectric sphere of radius $5nm$.
Source: The Authors.

The behavior of the transverse component and of the *Gradient Force* will be the same that in the component x, as is possible to observe in the equations (5) and (6), because of symmetry. In Fig. 2 it is possible to obtain a view in the transverse plane xy, where the origin of each arrow indicates the position of the sphere, the length of the arrow represents the magnitude of the *Gradient force* and the direction of the arrow represents the direction of the force respectively. In order to facilitate the analysis, the intensity of the beam has been recorded in the same figure and where it is possible to corroborate the previous restorative behavior in Fig. 1 of the transverse components of the *Gradient force*. In other words, a potential well is generated in the region of greater intensity of the beam.

In the Fig. 3, is possible to observe the behavior of the transverse component of the *Gradient Force* on the front plane *xz* and a cut of the intensity beam in its same plane. In the Fig. 3 is evident its restorative behavior at the zones in *x* where is to get the greater intensity beam. Nevertheless, is possible to observe that is force is more intensity in the Rayleigh's length ($\tilde{z} = 0{,}5$), which is the distance of propagation of beam in where the beam not diverge significantly and is taken since of beam waist.

In Fig. 4, is possible to observe the behavior of the longitudinal component *z* of the *Gradient Force,* in a front plane *xz.* This force positioned at sphere in the greater intensity beam that it is location in the region of beam waist ($\tilde{z} = 0$). This force is more intensity in the Rayleigh's length ($\tilde{z} = 0{,}5$) and is minor in a distance more far of this region. Thus, is possible to observe that on the axes of beam there not is contribution of the longitudinal component of the *Gradient Force*, because there is absence of radiation in the dark zone of the beam.

In Fig. 5, is observe the behavior of *Scattering Force* on a sphere that is positioned in $\tilde{z} = 1$ (Fig. 7) and in some positions on the transverse axes $\tilde{x}$. We observe that the values in the *Scattering Force* are always positive, permitting that sphere is accelerated in the direction of propagation beam. Is possible too to observe in Fig. 5 that the longitudinal component of the *Gradient Force* for $-2{,}2 < \tilde{x} < 0$, take negative values; which permited to transport sphere in opossite direction of propagation, for the zone of greater intensity, which localization is ($\tilde{z} = 0$).

This same behavior occur for $0 < \tilde{x} < 2{,}2$. Neverthless, is possible to observe that for $\tilde{x} < -2{,}2$ and for $\tilde{x} > 2{,}2$, the *Gradient force* push to the sphere in the direction of propagation beam. This behavior is because of that the *Gradient force* has restorative nature at to the zones more near of greater intensity of the beam, and as the sphere is encountered very close of dark zone (without radiation), the intensity zone more close is encountered in the direction propagation of beam. This phenomenon can be observed with more clarity Fig. 4 in $\tilde{z} = 0{,}5$ for $\tilde{x} < -1{,}5$ and for $\tilde{x} > 1{,}5$.

In the same Fig. 5, it can be evidenced the longitudinal component z of the *Total force*, that is the addition of longitudinal of the *Gradient force* and of the *Scattering force.* For $\tilde{z} = 1$, the longitudinal component of the *Total force* in $-2 < \tilde{x} < 0$, have negative values that indicate for this regions that the dielectric sphere is trapped and directed at the beam waist. This behavior is equal for $0 < \tilde{x} < 2$. Nevertheless, for $\tilde{x} < -2$ and for $\tilde{x} > 2$ the sphere is accelerated in the direction propagation of beam, phenomenon that is because of the *Gradient force*, explained a priori.

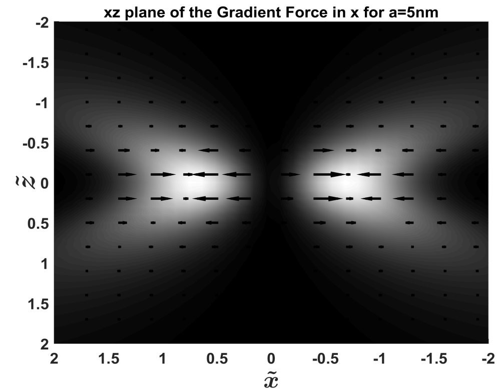

Figure 3. Front plane xz of the transverse component x of the Gradient Force for dielectric sphere of radius $5nm$.
Source: The Authors.

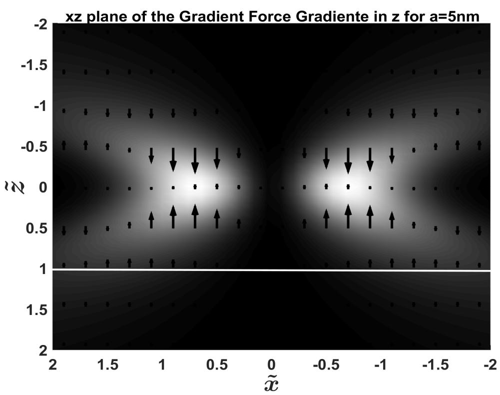

Figure 4. Front plane xz of the longitudinal component z of *Gradient force* for a dielectric sphere of radius $5nm$.
Source: The Authors.

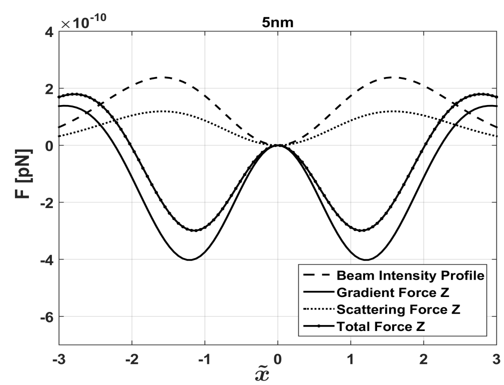

Figure 5. Longitudinal Component z of *Gradient force, Scattering* and *Total* in the transverse axe x for $\tilde{z} = 1$ for dielectric sphere of radius $5nm$.
Source: The Authors.

A qualitative analysis of the behavior of the *Gradient force* in the 3D space, can obtained in Fig. 6. In this figure, the hollow hyperboloid represent the zones of greater intensity of the mode TEM_{01}^{*}. Is possible evident the restorative nature of the *Gradient force*, at to regions of greater intensity. Nevertheless, is possible to observe that arrows that represent at the *Gradient force* only have components in the plane *xy*. This is because of that transverse components in x and y (Fig.1), are of order 10^{-7} while the longitudinal component z, is of order 10^{-10} (Fig. 5), and therefore, thousand times smaller than the transverse component.

This means that the vectors have an inclination with respect to the plane xy of $\theta \approx 0{,}0405$ that can not be appreciated in Fig. 6. As it is possible to predict, the sphere will experience a force that will position it in the regions more intense in the transverse plane *xy* and that will be much greater than the longitudinal effect.

In more detail, in Fig. 7 which corresponds to a frontal plane *xz*, it is possible to observe the accelerating behavior in the direction of propagation, which has the *Scattering force* on the sphere, and its direct proportionality with the intensity of beam. In addition, it should be specified that there is no *Scattering force* in the dark zone of the beam, which is due to the absence of radiation.

The Fig. 8 correspond to the *3D Scattering force* and permitted to observe that for each position of the space where is encountered the sphere this force is responsible of to accelerate to the sphere in the direction of propagation of beam. The maximum magnitude of this force is encountered in the greater intensity zones of beam.

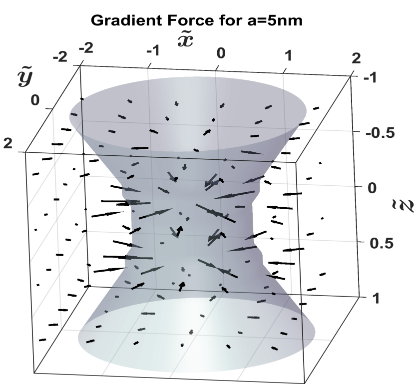

Figure 6. Vector field of the *Gradient force* for a dielectric sphere of radius $5nm$.
Source: The Authors.

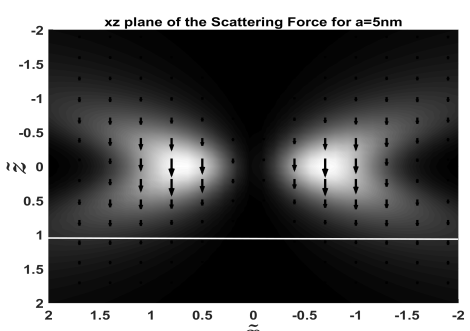

Figure 7. Front Plane xz of the *Scattering force* for a dielectric sphere of radius $5nm$.
Source: The Authors.

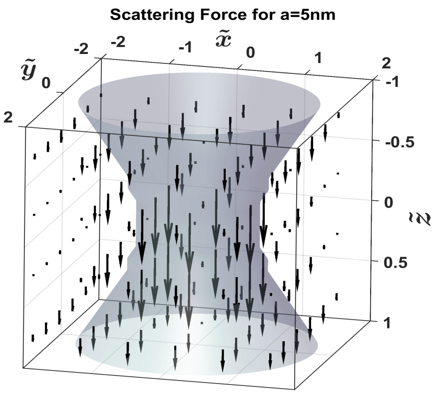

Figure 8. Vector field of the Scattering force for a dielectric sphere of radius $5nm$.
Source: The Authors.

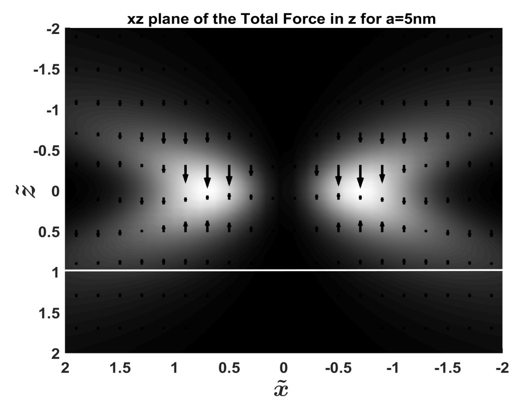

Figure 9. Front plane xz of the longitudinal component z of the *Total force* for dielectric sphere of radius $5nm$.
Source: The Authors.

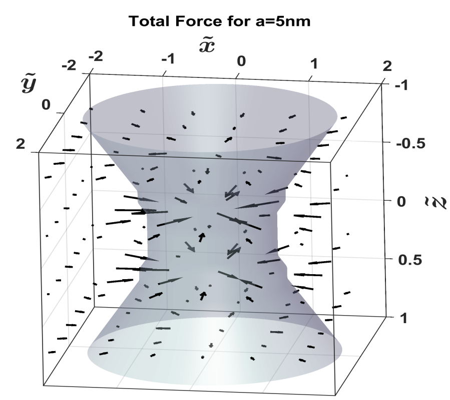

Figure 10. Vector field of the Total force for a dielectric sphere for radius $5nm$.
Source: The Authors.

In Fig. 9 it is possible to observe the longitudinal component of the *Total force*, corresponding to addiction of the *Scattering force* and the longitudinal component of the *Gradient force*. For when $\tilde{z} > 0$ the *Total force* change of direction, and have a magnitude that must face at to the *Gradient force* and *scattering force*, that is minor that in $\tilde{z} < 0$ which both components have the same direction.

The *Total force* in space will be the *Gradient force* in transverse plane xy and addition of its longitudinal component with the *Scattering force* which is possible to see in Fig. 10. In this figure is evident that under the parameters: refraction index, radius of the sphere, wavelength, beam waist and power of beam, is possible to observe a capture of the sphere in the ring of beam that is encountered in beam waist, establishing a potential well in this zone where the greater intensity is found, it should be noted that no *Total force* is present in the dark zone of the beam, as previously demonstrated. Finally, we could also observe that the arrows that represent the *Total force* are only on the xy plane, a phenomenon that is due to the difference in the order of the longitudinal component with respect to the transverse component.

4. Interface

To facilitate the analysis in the radiation forces, establishing different parameters, a graphical user interface was developed in MATLAB. This interface implements the equations developed previously with the approximations of Rayleigh Scattering Regime. This method uses equations of electrodynamics to have a theoretical, phenomenological idea and a notion closer what gives rise to the operation of the OT.

The developed interface has two options: 2D Analysis (Fig. 11) and 3D Analysis (Fig. 12), which allow observing the behavior of *Gradient, Scattering* and *Total forces* on some transverse and frontal planes, and in the 3D space respectively.

The interface has a panel for inputting parameters by the user which are: refractive index of the medium surrounding the sphere, refractive index of the sphere, radius of the sphere (*nm*), wavelength of the beam capture (*nm*), capture beam power in (*mW*), beam waist(μm).

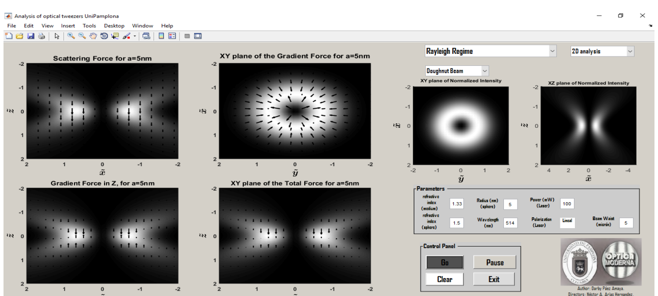

Figure 11. Graphical user interface, option for 2D visualization.
Source: The Authors.

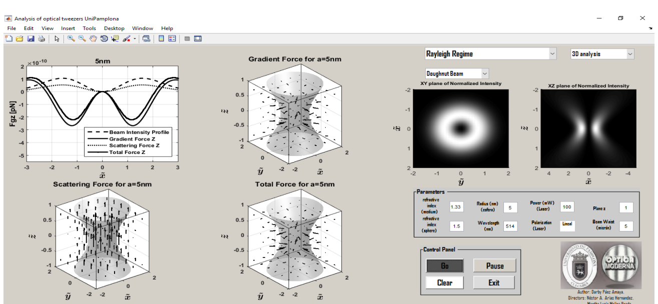

Figure 12. Graphical user interface, option for 3D visualization.
Source: The Authors.

5. Conclusions

In this work, we presented math expressions for Gradient and Scattering forces exerted on a dielectric sphere under illumination for TEM_{01}^{*} mode linearly polarized under Rayleigh approach.

Our results under this approximation, can be firstly used by the understanding of behavior in trapping microbead of optical force profile generated by complex beams, e.g. the TEM_{01}^{*} mode beam.

To show and study the behavior of radiation forces we realized graphical comparisons in the longitudinal, transverse components and vector field. In addition, we developed a GUIDE in MATLAB to study the radiation forces easier when a user changes the trapping parameters.

Acknowledges

This research was done by Metrology Laboratory of group of modern optic (GOM) of University of Pamplona and under the grants: PR400-156.012-010(GA313-BE-2016). The authors acknowledge financial support of the Vicerrectoría de Investigaciones de la Universidad de Pamplona (Pamplona-Colombia).

Appendix

If we used the vector identity

$$\boldsymbol{\nabla}(\boldsymbol{A}.\boldsymbol{B}) = (\boldsymbol{B}.\boldsymbol{\nabla})\boldsymbol{A} + (\boldsymbol{A}.\boldsymbol{\nabla})\boldsymbol{B} + \boldsymbol{B}\times(\boldsymbol{\nabla}\times\boldsymbol{A}) + \boldsymbol{A}\times(\boldsymbol{\nabla}\times\boldsymbol{B}), \quad (11)$$

In addition, using $\boldsymbol{E}(\boldsymbol{r},t)$ is possible to show that

$$[\boldsymbol{E}(\boldsymbol{r},t).\boldsymbol{\nabla}]\boldsymbol{E}(\boldsymbol{r},t) = \frac{1}{2}\boldsymbol{\nabla}E^2(r,t) + \boldsymbol{E}(\boldsymbol{r},t)\times[-\boldsymbol{\nabla}\times\boldsymbol{E}(\boldsymbol{r},t)], \quad (12)$$

Substituting the Eq.1 into Eq. 12 and with Faraday's law

$$[\boldsymbol{p}.\boldsymbol{\nabla}]\boldsymbol{E}(\boldsymbol{r},t) = 4\pi n_m^2\varepsilon_0 a^3\left(\frac{m^2-1}{m^2+2}\right)\left[\frac{1}{2}\boldsymbol{\nabla}E^2(r,t) + \boldsymbol{E}(\boldsymbol{r},t)\times\frac{d\boldsymbol{B}(\boldsymbol{r},t)}{dt}\right] \quad (13)$$

Now, with the Eq. 13, we can modify the math expression in Eq. 2 to write

$$\boldsymbol{F}_{Neta}(\boldsymbol{r},t) = 4\pi n_m^2\varepsilon_0 a^3\left(\frac{m^2-1}{m^2+2}\right)\left[\frac{1}{2}\boldsymbol{\nabla}E^2(r,t) + \boldsymbol{E}(\boldsymbol{r},t)\times\frac{d\boldsymbol{B}(\boldsymbol{r},t)}{dt}\right] + \frac{d\left(4\pi n_m^2\varepsilon_0 a^3\left(\frac{m^2-1}{m^2+2}\right)\boldsymbol{E}(\boldsymbol{r},t)\right)}{dt}\times\boldsymbol{B}(\boldsymbol{r},t) \quad (14)$$

A math equation simpler than Eq. 14 you can achieve if used the derivative applied at cross product between two vectors in the last two terms of Eq. 14, so

$$\langle \boldsymbol{F}_{Neta}(r,t)\rangle_T = 4\pi n_m^2 \varepsilon_0 a^3 \left(\frac{m^2-1}{m^2+2}\right)\left\{\frac{1}{2}\boldsymbol{\nabla}E^2(r,t) + \frac{d}{dt}[\boldsymbol{E}(\boldsymbol{r},t)\times \boldsymbol{B}(\boldsymbol{r},t)]\right\}, \tag{15}$$

If the laser power is constant in all the time, the temporal derivative of Poynting Vector its worth zero, then

$$\boldsymbol{F}_{Neta}(\boldsymbol{r},t) = 4\pi n_m^2 \varepsilon_0 a^3 \left(\frac{m^2-1}{m^2+2}\right)\left[\frac{1}{2}\boldsymbol{\nabla}E^2(r,t)\right] \tag{16}$$

The electric field is varying very fast in the time, and then temporal average must be used, so, $\langle E^2(r,t)\rangle_{\boldsymbol{T}} = \frac{\mathbf{1}}{\mathbf{2}}|E(r)|^{\mathbf{2}}$ and the intensity of electromagnetic wave $I(r) = \frac{c\varepsilon_0 n_m}{2}|E(r,t)|^{\mathbf{2}}$ are used to reduce the Eq. 16 finally (as Eq. 3)

$$\langle \boldsymbol{F}_{Neta}(r,t)\rangle_T = \boldsymbol{F}_G(r) = \frac{2\pi n_m a^3}{c}\left[\frac{m^2-1}{m^2+2}\right]\boldsymbol{\nabla}\mathrm{I}(r) \tag{17}$$

References

[1] Ashkin, A., Acceleration and trapping of particles by radiation pressure. Phys. Rev. Lett., 24(4), pp. 156-159, 1970. DOI: 10.1103/PhysRevLett.24.156

[2] Baumann, C.G., Smith, S.B., Bloomfield, V.A. and Bustamante, C., Ionic effects on the elasticity of single DNA molecules, Proceedings of the National Academy of Sciences, 94(12), pp. 6185-6190, 1997. DOI: 10.1073/pnas.94.12.6185

[3] Svoboda, K., Schmidt, C.F., Schnapp, B.J. and Block, S.M., Direct observation of kinesin stepping by optical trapping interferometry. Nature, 365(6448), pp. 721-727, 1993. DOI: 10.1038/365721a0

[4] Català, F., Marsà, F., Montes-Usategui M., Farré, A. and Martín-Badosa, E., Influence of experimental parameters on the laser heating of an optical trap., Scientific Reports, 7(1), pp. 1-9, 2017. DOI: 10.1038/s41598-017-15904-6

[5] Padgett, M. and Bowman, R., Tweezers with a twist. Nature Photonics, 5, pp. 343-348, 2011. DOI: 10.1038/nphoton.2011.81

[6] Zhou, L.M., Xiao, K.W., Chen, J. and Zhao, N., Optical levitation of nanodiamonds by doughnut beams in vacuum. Laser and Photonics Reviews, 11(2), pp. 1-8, 2017. DOI: 10.1002/lpor.201600284

[7] Zhou, X., Chen, Z., Liu, Z. and Pu, J., Experimental investigation on optical vortex tweezers for microbubble trapping. Open Physics, 16(1), pp. 383-386, 2018. DOI: 10.1515/phys-2018-0052

[8] Zhang, D.W. and Yuan, X.C., Optical doughnut for optical tweezers. Opt. Lett. 28(9), pp. 740-742, 2003. DOI: 10.1364/OL.28.000740

[9] Dasgupta, R., Ahlawat, S., Verma, R.S., Shukla, S. and Gupta, P.K., Optical trapping of spermatozoa using Laguerre-Gaussian laser modes. Journal of Biomedical Optics, 15(6), pp. 1-5, 2010. DOI: 10.1117/1.3526362

[10] Harada, Y. and Asakura, T., Radiation forces on a dielectric sphere in the Rayleigh scattering regime. Optics Communications, 124(5), pp. 529-541, 1996. DOI: 10.1016/0030-4018(95)00753-9

[11] Paez-Amaya, D., Análisis teórico de las pinzas ópticas bajo las aproximaciones de Rayleigh y Mie, Tesis de Pregrado, Departamento de Física y Geología, Universidad de Pamplona, Pamplona, Colombia, 2015.

[12] Páez-Amaya, D., Arias-Hernandez, N.A. and Molina-Prado, M.L., Interfaz gráfica para el análisis de las fuerzas de captura en una pinza óptica usando las aproximaciones de Rayleigh y Mie. Bistua: Revista de la Facultad de Ciencias Básicas, 14(2), pp. 182-193, 2016. DOI: 10.24054/01204211.v2.n2.2016.2192

[13] Jackson, J.D., Classical Electrodynamics. John Wiley & Sons, Inc, 3rd Ed., California, USA, 1999.

[14] Allen, L., Beijersbergen, M.W., Spreeuw, R.J.C. and Woerdman, J.P., Orbital angular momentum of light and the transformation of Laguerre-Gaussian laser modes. Phys. Rev. A., 45(11), pp. 8185-8189, 1992. DOI: 10.1103/PhysRevA.45.8185

[15] Siegman, A.E., Lasers. University Science Books, California, USA, 1986.

[16] Bahaa E. A. Saleh. Fundamentals of photonics. California: John Wiley & Sons, Inc, 1991.

[17] Andrews, L.C. and Phillips R.L., Laser beam propagation through random media, SPIE, Washington, USA, 2005.

[18] Tsang, L., Kong, J.A. and Ding K.-H., Scattering of electromagnetic waves: theories and applications, John Wiley & Sons, Inc, California, USA, 2000.

D. Paez-Amaya, received the BSc. in Physics in 2015, MSc. in Physics in 2019, all of them from the Universidad de Pamplona, Colombia. He has worked as a professor and researcher for over three years. Currently, he is occasional-time professor in the Physics Program, Faculty of Natural Sciences, Universidad de Pamplona, Pamplona, Colombia. His research interests include: optics, optical design and optical tweezers.
ORCID: 0000-0002-2204-5344

M.L. Molina-Prado, received the BSc. in Mathematic and Physics in 1994, from the Universidad Popular del Cesar, Colombia, MSc in Physics in 2003, from the Universidad Industrial de Santander, Colombia, PhD. in natural sciences (Physics) in 2010, from the Universidad Industrial de Santander, Colombia. She has worked as a professor and researcher for over fifteen years. Currently, she is a full professor in the Physics Program, Faculty of Natural Sciences, Universidad de Pamplona, Pamplona, Colombia. Her research interests include: optics, speckle metrology and photorefractive crystals.
ORCID: 0000-0002-3347-7986

N.A. Arias-Hernández, received the BSc. in Mathematical and Physics in 1994, from the Universidad Popular del Cesar, Colombia, MSc. in Physics in 2004, from the Universidad Industrial de Santander, Colombia, PhD. degree in natural sciences (Physics) in 2010. He has worked as a professor and researcher for over fifteen years. Currently, he is a full professor in the Physics Program, Faculty of Natural Sciences, Universidad de Pamplona, Pamplona, Colombia. His research interests include: optics, image processing, optical design and optical metrology.
ORCID: 0000-0002-9224-7654